IEEE Photonics Journal
An IEEE Photonics Society Publication

Open Access

Strain Sensor Based on Fiber Ring Cavity Laser With Photonic Crystal Fiber In-Line Mach–Zehnder Interferometer

Volume 6, Number 4, August 2014

Xuekun Bai
Dengfeng Fan
Shaofei Wang
Shengli Pu
Xianglong Zeng

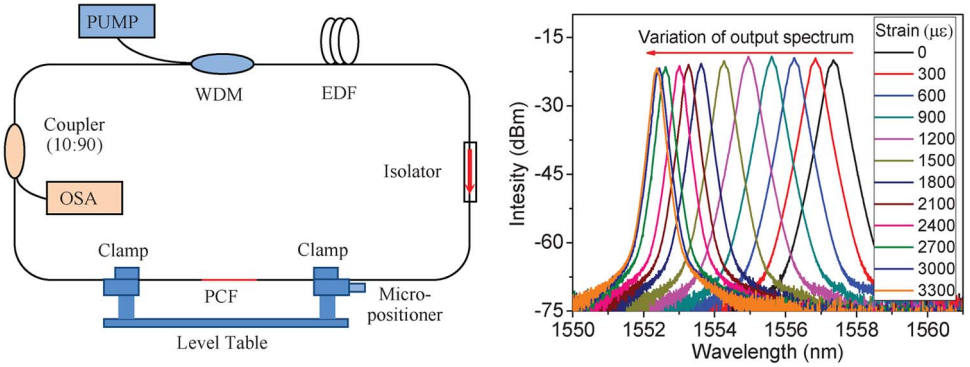

DOI: 10.1109/JPHOT.2014.2332454
1943-0655 © 2014 IEEE

Strain Sensor Based on Fiber Ring Cavity Laser With Photonic Crystal Fiber In-Line Mach–Zehnder Interferometer

Xuekun Bai,[1] Dengfeng Fan,[1] Shaofei Wang,[1] Shengli Pu,[2] and Xianglong Zeng[1]

[1]The Key Lab of Specialty Fiber Optics and Optical Access Network, Shanghai University, Shanghai 200072, China
[2]College of Science, University of Shanghai for Science and Technology, Shanghai 200093, China

DOI: 10.1109/JPHOT.2014.2332454

Manuscript received May 9, 2014; revised June 15, 2014; accepted June 17, 2014. Date of publication June 24, 2014; date of current version July 9, 2014. This work was supported in part by the National Natural Science Foundation of China under Grant 11274224, by the Shanghai Shuguang Program under Grant 10SG38, and by the State Key Laboratory Advanced Optical Communication System and Networks, Shanghai Jiaotong University, through an open program under Grant 2013GZKF031307. The work of X. Zeng was supported by the Program for Professor of Special Appointment (Eastern Scholar) at Shanghai Institutions of Higher Learning. Corresponding authors: S. Pu and X. Zeng (e-mail: shlpu@usst.edu.cn; zenglong@shu.edu.cn).

Abstract: We experimentally demonstrated a strain sensor based on fiber ring cavity laser with a photonic crystal fiber (PCF) in-line Mach–Zehnder interferometer (MZI) structure, which is used as an optical band-pass filter and acts as the strain sensing component. The fiber ring cavity laser plays the role of enhancing the visibility of the resonant spectrum and narrowing the corresponding 3-dB bandwidth, thus improving the comprehensive sensing performance. The induced axial strain on the structure is measured by monitoring the central wavelengths of the laser output. A high strain sensing sensitivity of 2.1 pm/$\mu\varepsilon$ is successfully achieved in the linear strain range of 0–2100 $\mu\varepsilon$. A parameter Q value describing the overall sensing performance is introduced by including the strain sensing sensitivity, sensing sensitivity relative to 3-dB bandwidth of the resonant spectrum and the corresponding visibility. Comparing with the reported strain measurements based on a PCF in-line MZI structure, the experimental results based on fiber ring cavity laser sensor present more than nine times larger Q value.

Index Terms: Strain sensors, fiber lasers, in-line Mach-Zehnder interferometer, fiber optics systems.

1. Introduction

Optical fiber sensors have attracted great research interests and been widely used to sense temperature [1], [2], magnetic field [3], [4], chemical gas [5], liquid concentration [6], surrounding refractive index [7], curvature [8] or others factors due to their unique advantages of compact size, low cost, high sensitivity, and immunity to electromagnetic interference. As an effective way of in-situ monitoring in the application of health inspection of large buildings such as bridges and dams, optical fiber sensor is usually used to measure strain. Several types of optical fiber strain sensors have been proposed, such as fiber Bragg gratings [9]–[12], Fabry–Perot interferometer [13], microfiber in-line Mach–Zehnder interferometer [14], and strain sensors based on multimode interference [15]–[18]. These optical fiber strain sensors

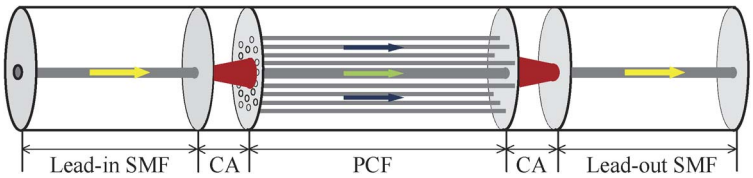

Fig. 1. Schematic diagram of the proposed PMS.

exhibit good performance in sensing strain. However, the cross sensitivity between strain and temperature is one of the critical problems, which requires further necessary treatment of temperature calibration.

Photonic crystal fiber (PCF) as a new sensing media presents a low thermo-optical coefficient because of the array of air holes distributed longitudinally along the fiber. The temperature insensitive strain sensors based on PCF in-line Mach-Zehnder interferometer (MZI) have been proposed [19]–[23]. Such strain sensors based on PCF in-line MZI structure (PMS) have advantages of high sensitivity, simple manufacturing technology and compact structure. But the visibility (the spectral transmission difference between a peak and its adjacent dip) of the response spectrum is relatively low and its 3-dB bandwidth is usually wide due to the limited interference effect between the core and cladding modes. The strain is measured usually by monitoring the change of the dip central wavelengths. So the accuracy and resolution will be reduced by the low quality of the response spectrum. Recently, some fiber laser strain sensing systems have been demonstrated [24]–[26] with high visibility and narrow bandwidth, which possess the inherent high sensing accuracy and resolution. In these schemes, monitoring the beat frequency or the wavelength shift is usually utilized to measure the strain dynamically.

In this paper, we take advantage of the temperature insensitivity PMS in a fiber ring cavity laser strain sensor. The PMS is used as optical band-pass filter of the laser cavity and acts as a strain sensing component. The fiber ring cavity plays a role of lasing signal which contains the information of induced strain on the structure. High strain sensing sensitivity (2.1 $pm/\mu\varepsilon$), high visibility (45 dB) and narrow 3-dB bandwidth (0.3 nm) are achieved using this fiber ring cavity laser strain sensing method. A dimensionless quality factor Q value is defined to describe the sensing comprehensive performance including the sensitivity, accuracy and resolution.

2. Basic Principle of the Strain Sensing Based on PMS

Fig. 1 illustrates a schematic diagram of the proposed PMS. A section of PCF is spliced between two standard single mode fibers (SMFs), i.e., the lead-in and the lead-out SMFs. Two collapsing areas (CAs) are created at the two spliced joints when splicing SMFs with PCF. Inside the CA, the incident light is divided into the core and cladding modes of PCF and recombined in the lead-out SMF, resulting in an interference pattern.

The intensities of the core and cladding modes are $I_1(\lambda)$ and $I_2(\lambda)$. $I(\lambda)$ is the intensity of incident fundamental mode. γ is defined as the ratio of fundamental mode emitted into the core and the cladding modes of the PCF at the lead-in spliced joint. So the intensities of core and cladding modes can be expressed as $I_1(\lambda) = \gamma I(\lambda)$ and $I_2(\lambda) = (1-\gamma)I(\lambda)$. The output interference intensity from the lead-out SMF is

$$I_{out} = I(\lambda)\left[1 + 2\sqrt{\gamma(1-\gamma)}\cos(\phi)\right] \tag{1}$$

where ϕ is the phase difference between the core and cladding modes in the PCF and can be approximated as $\phi = 2\pi\Delta n_{eff}L/\lambda$, Δn_{eff} is the effective refractive index difference between the core and cladding modes, L is the PCF length and λ is the light wavelength in vacuum. When ϕ satisfies $\phi = 2m\pi$, where m is an integer, the transmitted intensity peaks appear at the

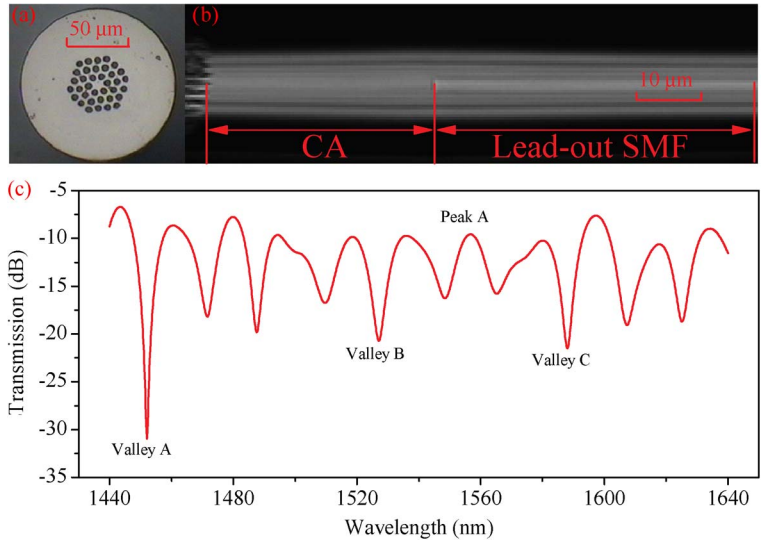

Fig. 2. (a) The microscope image of PCF cross section. (b) CA between PCF and Lead-out SMF. (c) Transmission spectrum of PMS.

wavelengths: $\lambda_{peak} = \Delta n_{eff} L/m$. By differentiating λ_{peak} with respect to L, the m_{th} peak wavelength shift can be given as [27]

$$\Delta\lambda_m = \left[1 + \left(\frac{L}{\Delta_{n_{eff}}}\right) \cdot \left(\frac{\partial(\Delta_{n_{eff}})}{\partial L}\right)\right] \lambda_m \varepsilon. \tag{2}$$

It is known that the wavelength shift caused by the induced strain on PMS is a linear function of the corresponding strain in an appropriate range. The dip wavelength shift also shows the similar trend. From (2), the strain sensing sensitivity can be obtained as

$$S = \frac{\Delta\lambda_m}{\varepsilon} = \left[1 + \left(\frac{L}{\Delta_{n_{eff}}}\right) \cdot \left(\frac{\partial(\Delta_{n_{eff}})}{\partial L}\right)\right] \lambda_m. \tag{3}$$

So, it can be found that the strain sensitivity S only depends on the change of Δn_{eff} caused by the extended PCF length L $(\partial(\Delta n_{eff})/\partial L)$ when there is a strain induced on the PMS from (3). From (1), we can find that the output intensity only depends on the ratio γ at the dips or peaks of interference fringe when the incident intensity is constant. The axial strain on the PMS would induce a slight physical deformation of the spliced joint. So, the ratio γ and the output intensity could change slightly.

3. Experiments and Results

3.1. Fabrication of PMS

A section of PCF (YSL photonics SM-10 PCF) with a length of 15 mm is spliced between two SMFs (Corning SMF-28) by using a commercial splicer (Fujikura FSM-100P+). The microscope image cross section of PCF is shown in Fig. 2(a). CAs are observed at the spliced joints, as shown in Fig. 2(b). During the splicing process, the overlay of PCF and SMFs, the arc discharge intensity and time need to be carefully adjusted via the hand mode of the splicer to get the highest visibility of 23 dB in the resonant spectrum, as shown in Fig. 2(c). In this study, we set the according parameters for splicing SMF and PCF as follow: overlay distance: 45 μm, main discharge power: 293 bit, main discharging time: 2100 ms. More than one cladding modes are excited in the collapsing area between the lead-in SMF and PCF. Therefore, more than one frequency components can be observed in the interference fringe. As a result, the fringe is not

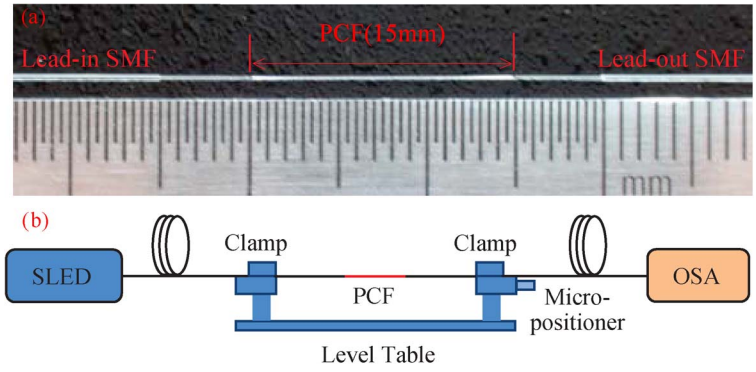

Fig. 3. (a) The PMS used in this experiment. (b) Experimental setup for PMS based strain sensor.

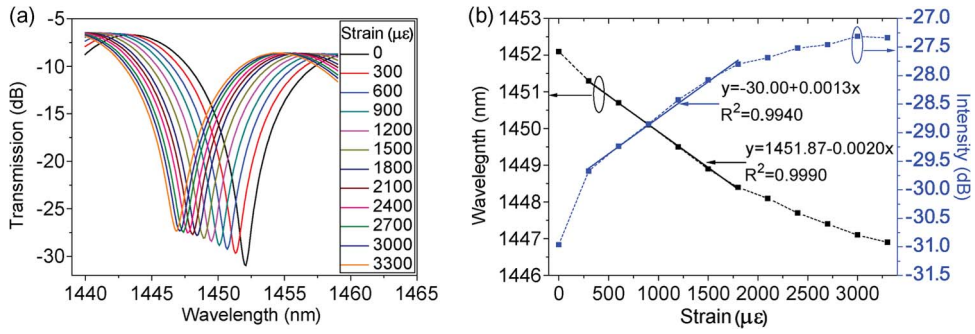

Fig. 4. (a) Interference fringes of the PMS with different strain. (b) Dip wavelenght and intensity versus tensile strain.

uniform, and the extinction ratio changes with the wavelength [19], [20], [22] [see Fig. 2(c)]. It is found the PMS has an insertion loss of nearly -6.7 dB from Fig. 2(c).

3.2. Strain Sensing Based on PMS

The PMS and the experimental setup for the strain sensor based on the PMS are shown in Fig. 3(a) and (b), respectively. A 1550 nm wavelength super luminescent diode (SLED) (B&A Technology, SL3215-1550) and an optical spectrum analyzer (OSA) (YOKOGAWA, AQ6370C) are connected with the lead-in and lead-out SMFs, respectively. The PMS is fixed by two clamps placed on a level table, and the distance between two clamps is 33.3 cm. The axial strain is induced on the PMS by rotating the micro-positioner (precision: 10 μm) of the right clamp at a step of 50 μm which converts into the axial strain of 150 $\mu\varepsilon$.

Considering the different visibility and 3-dB bandwidth of the resonant spectrum, the wavelength shifts of valley A, B, and C (labeled in Fig. 2(c)) are selected to study the strain sensing properties based on the PMS comparatively. A typical interference fringe of valley A with different tensile strain is illustrated in Fig. 4(a), and the center dip wavelengths and intensities versus the strain are shown in Fig. 4(b).

When the tensile strain is induced on the PMS, according to the analysis of Section 2, the dip wavelength reduces as the strain increases. As shown in Fig. 4(a) the dip wavelength decreases from 1452.1 nm to 1446.9 nm and the strain sensitivity of 2.0 pm/$\mu\varepsilon$ is achieved in a linear strain sensing range of 300–1800 $\mu\varepsilon$. But the strain sensitivity reduces a little when the strain exceeds 2100 $\mu\varepsilon$ (see Fig. 4(b). The physical deformation of PMS would be approaching the saturated value when the induced strain is big enough. Then, the change of Δn_{eff} caused by the extended PCF length L $(\partial(\Delta n_{eff})/\partial L)$ would be reduced. So, according to (3), the

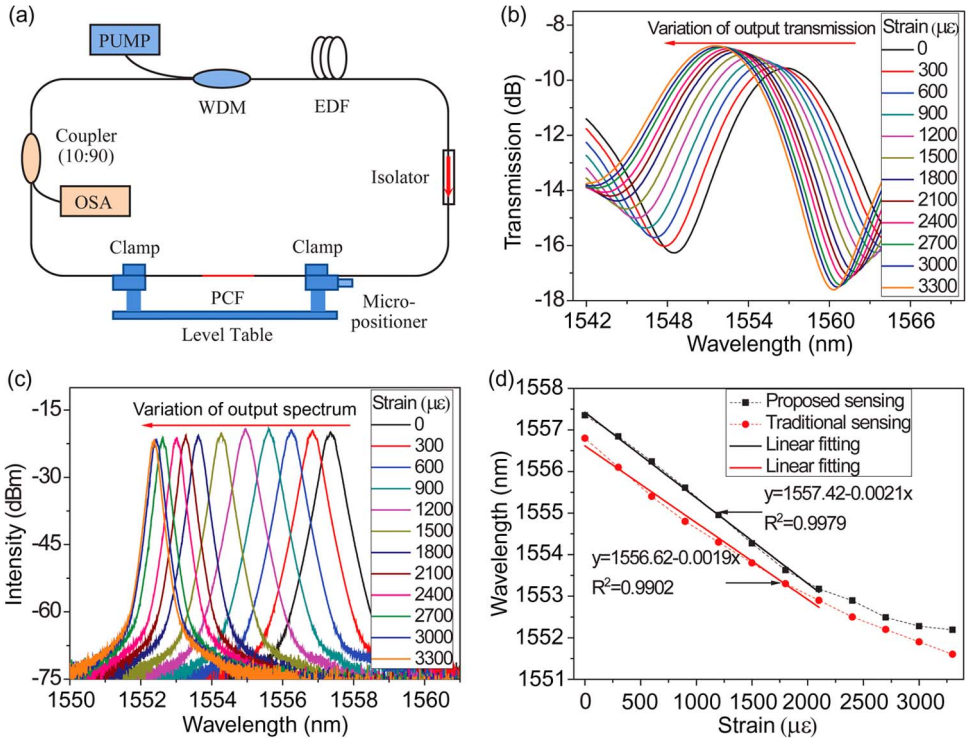

Fig. 5. (a) Experimental setup of the fiber ring laser with PMS, spectral response against the axial strain for (b) PMS based sensor, and (c) the proposed fiber ring cavity laser strain sensor. (d) Measured central wavelenght shift vs. axial strain.

strain sensitivity would reduce for relatively big induced strain. The intensity variation sensitivity of 0.0013 dB/$\mu\varepsilon$ is obtained in the linear range 300–1800 $\mu\varepsilon$, which is relatively low compared with the one in reference [28] 0.023 dB/$\mu\varepsilon$. The above strain measurements have good repeatability because of the simple and compact PMS, the strong strength of the spliced joints. The strain sensitivity obtained from Valley B and Valley C are 2.02 pm/$\mu\varepsilon$ and 2.08 pm/$\mu\varepsilon$, respectively. The visibility of the interference fringes are 17.6 dB, 10.2 dB, and 9.3 dB for Valley A, Valley B, and Valley C, respectively, and their corresponding 3-dB bandwidth are 0.8 nm, 3.2 nm, and 2.5 nm. These strain sensitivities based on the PMS are comparable to or even better than those reported in reference [20] (1.84 pm/$\mu\varepsilon$), [21] (0.31 pm/$\mu\varepsilon$) and [22] (2.1 pm/$\mu\varepsilon$).

3.3. Strain Sensing Based on Fiber Ring Cavity Laser with PMS

In order to improve the comprehensive sensing performance of the PMS strain sensor, especially enhance the visibility of the response spectrum and reduce the corresponding 3-dB bandwidth, a strain fiber ring cavity laser sensor based on the PMS is proposed and experimentally investigated as shown in Fig. 5(a). It is composed of a 980 nm pump light source, a section of Er-doped fiber, a wavelength division multiplexer (WDM), and a PMS fixed by two clamps. A C-band isolator is inserted into the fiber ring cavity for the unidirectional light, and a 10:90 coupler is employed to lead out the laser light for wavelength monitoring. A band-pass filter (1550–1562 nm) in the transmission spectrum is marked as peak A in Fig. 2(c), which ensures fiber lasing at the central wavelength of Peak A. The spectra corresponding to different strain using the PMS transmission (Peak A) and ring cavity laser sensing are shown in Fig. 5(b) and (c), respectively.

The transmission spectrum of the PMS and the lasing wavelengths blueshift with the increase of the axial strain, which is shown in Fig. 5(b) and (c). The central wavelength variations as a function of axial strain are plotted in Fig. 5(d). The central wavelength decreases monotonically

TABLE 1

The Q value of different sensing ways

Sensing Way	Valley A	Valley B	Valley C	Peak A	FL-PM
Q	92.7	13	16.1	2.0	661.5

TABLE 2

Comparison between the reported strain sensors based on PMS and this study, where all the wavelengths are around 1550 nm

Ref.	Visibility (dB)	Sensitivity ($pm/\mu\varepsilon$)	3-dB bandwidth (nm)	Q Value	Length (mm)
[19]	8	2.26	4	10.2	120
[20]	7.5	1.84	7	3.6	7
[21]	11	0.31	0.3	3.5	100
[22]	12	2.1	1	52.9	45
$[FL-PM]$	45	2.1	0.3	661.5	15

with the induced strain on the structure. A linear fitting to the experimental results presents a strain sensing sensitivity of 1.9 pm/$\mu\varepsilon$ and 2.1 pm/$\mu\varepsilon$ in the range of 0–2100 $\mu\varepsilon$, which reveals a good agreement between the center wavelength of PMS filter (Peak A) and the fiber ring cavity laser output. The R^2 values of 0.9979 and 0.9902 indicate that the proposed fiber ring cavity laser based on the PMS sensor is more accurate. When the strain exceeds 2100 $\mu\varepsilon$, the strain sensitivity reduces a little because of the strain approaching the saturated value. A higher visibility ($\sim$45 dB) and narrower 3-dB bandwidth ($\sim$0.3 nm) of the resonant spectrum [see Fig. 5(c)] are obtained with the fiber ring cavity laser sensor, compared to the visibility ($\sim$5.2 dB) and 3-dB bandwidth ($\sim$9.2 nm) with the PMS sensing structure shown in Fig. 5(b). The sensitivity, visibility and 3-dB bandwidth of this strain sensing spectrum could be further improved via optimizing the system parameters, such as the fabrication of PMS, the selection of working wavelength, the amplification of the fiber laser and the length of PCF. The resolution of the OSA used in this experiment is 20 pm, so the detection limit of 9.5 $\mu\varepsilon$ is achieved.

4. Discussion

Considering the comprehensive sensing properties of the strain sensor, a quality factor Q value is defined in this paper. High sensitivity is usually preferable in practical application. If strain sensitivity (S) is much smaller than the 3-dB bandwidth ($FWHM$) of the resonance dip or peak, the sensing resolution would be low. Higher visibility (V) means a higher sensing accuracy. Hence, the product of S, $S/FWHM$, and V can be used to express the Q value

$$Q = K \cdot S \cdot S/FWHM \cdot V = KS^2V/FWHM \tag{4}$$

where the K is a unit coefficient with $\varepsilon^2/(\text{nm} \cdot \text{dB})$ to normalize the physical dimension. Then the Q value is just a constant without dimension, and used to describe the comprehensive sensing quality including the sensing sensitivity, resolution and accuracy. The corresponding Q value of strain sensing with the PMS based on Valley A, Valley B, Valley C, Peak A, and the Q value of fiber ring cavity laser strain sensor with PMS (FL-PM) are presented in Table 1.

Compared with the strain sensing based on the peak of transmission spectrum (Peak A), the Q value of strain sensing based on fiber ring cavity laser with a PMS improves nearly 330 times, and has enhanced more than 7 times compared with the traditional strain sensing using the dip transmission spectrum (Valley A). The more detailed comparison between the corresponding experimental results in references and this study is shown in Table 2. We can find that the strain sensor based on fiber ring cavity laser with a PMS has more than 9 times Q value. It means that the strain sensor based on a fiber ring cavity laser improves the comprehensive sensing quality. That is mainly because the fiber ring cavity laser enhances the visibility of resonant spectrum and narrow the corresponding 3-dB bandwidth by using its amplification and

wavelength selection. Compared with the length of strain sensing component in [19], [21], [22], the proposed fiber ring cavity laser strain sensor component has a compact structure, i.e., the length of PCF used in that cavity is just 15 mm.

The PCF used in this experiment consists of a pure-silica core with a diameter of 9.5 μm and three layers air holes with a diameter of 5.8 μm. It has a low thermo-optical coefficient. According to the results [20]–[22], the temperature sensitivity of this kind of PMS should be very low and can be neglected when it is operated in normal environmental condition without very large temperature variations.

5. Conclusion

In summary, a fiber ring cavity laser axial strain sensor based on PMS is studied experimentally. A high sensitivity of 2.1 pm/$\mu\varepsilon$ is achieved within a linear sensing range from 0 to 2100 $\mu\varepsilon$, functioned with the varied lasing central wavelength from 1557.352 nm to 1553.176 nm. Moreover, comparing with the reported strain sensing measurement using the PMS, the comprehensive quality (Q value) of this new strain sensor is improved more than 9 times. For the high sensing comprehensive quality, this new fiber laser strain sensor is valuable in application of a more exactness strain measurement and potential applications in long-distance axial strain sensing system.

References

[1] L. V. Nguyen, D. Hwang, S. Moon, D. S. Moon, and Y. Chung, "High temperature fiber sensor with high sensitivity based on core diameter mismatch," *Opt. Exp.*, vol. 16, no. 15, pp. 11 369–11 375, Jul. 2008.

[2] T. D. Vo *et al.*, "Chalcogenide fiber-based distributed temperature sensor with sub-centimeter spatial resolution and enhanced accuracy," *Opt. Exp.*, vol. 22, no. 2, pp. 1560–1568, Jan. 2014.

[3] A. Candiani *et al.*, "Magnetic field sensor based on backscattered intensity using ferrofluid," *IEEE Photon. Technol. Lett.*, vol. 25, no. 15, pp. 1481–1484, Aug. 2013.

[4] H. T. Wang, S. L. Pu, N. Wang, S. H. Dong, and J. Huang, "Magnetic field sensing based on singlemode–multimode–singlemode fiber structures using magnetic fluids as cladding," *Opt. Lett.*, vol. 38, no. 19, pp. 3765–3768, Oct. 2013.

[5] X. Lan *et al.*, "Fiber ring laser interrogated zeolite-coated singlemode–multimode–singlemode structure for trace chemical detection," *Opt. Lett.*, vol. 37, no. 11, pp. 1998–2000, Jun. 2012.

[6] Y. Zhao, Z. Q. Deng, and Q. Wang, "Fiber optic SPR sensor for liquid concentration measurement," *Sens. Actuators B, Chem.*, vol. 192, pp. 229–233, Mar. 2014.

[7] S. C. Warren-Smith and T. M. Monro, "Exposed core microstructured optical fiber Bragg gratings: Refractive index sensing," *Opt. Exp.*, vol. 22, no. 2, pp. 1480–1489, Jan. 2014.

[8] H. P. Gong, X. Yang, K. Ni, C. L. Zhao, and X. Y. Dong, "An optical fiber curvature sensor based on two peanut-shape structures modal interferometer," *IEEE Photon. Technol. Lett.*, vol. 26, no. 1, pp. 22–24, Jan. 2014.

[9] H. Y. Choi, K. S. Park, and B. H. Lee, "Photonic crystal fiber interferometer composed of a long period fiber grating and one point collapsing of air holes," *Opt. Lett.*, vol. 33, no. 8, pp. 812–814, Apr. 2008.

[10] M.-S. Yoon, S. Park, and Y.-G. Han, "Simultaneous measurement of strain and temperature by using a microtapered fiber grating," *J. Lightw. Technol.*, vol. 30, no. 8, pp. 1156–1160, Apr. 2012.

[11] C. E. Campanella *et al.*, "Localized strain sensing with fiber Bragg-grating ring cavities," *Opt. Exp.*, vol. 21, no. 24, pp. 29 435–29 441, Dec. 2013.

[12] H. R. Alemohammad, E. Foroozmehr, B. S. Cotten, and E. Toyserkani, "A dual-parameter optical fiber sensor for concurrent strain and temperature measurement: Design, fabrication, packaging, and calibration," *J. Lightw. Technol.*, vol. 31, no. 8, pp. 1198–1204, Apr. 2013.

[13] Y. Gong *et al.*, "Highly sensitive force sensor based on optical microfiber asymmetrical Fabry–Perot interferometer," *Opt. Exp.*, vol. 22, no. 3, pp. 3578–3584, Feb. 2014.

[14] C. Liao, D. Wang, and Y. Wang, "Microfiber in-line Mach–Zehnder interferometer for strain sensing," *Opt. Lett.*, vol. 38, no. 5, pp. 757–759, Mar. 2013.

[15] Q. Wang and G. Farrell, "All-fiber multimode-interference-based refractometer sensor: Proposal and design," *Opt. Lett.*, vol. 31, no. 3, pp. 317–319, Feb. 2006.

[16] S. M. Tripathi *et al.*, "Strain and temperature sensing characteristics of single-mode–multimode–single-mode structures," *J. Lightw. Technol.*, vol. 27, no. 13, pp. 2348–2356, Jul. 2009.

[17] A. M. Hatta, Y. Semenova, Q. Wu, and G. Farrell, "Strain sensor based on a pair of single-mode–multimode–single-mode fiber structures in a ratiometric power measurement scheme," *Appl. Opt.*, vol. 49, no. 3, pp. 536–541, Jan. 2010.

[18] J. Huang *et al.*, "Polymer optical fiber for large strain measurement based on multimode interference," *Opt. Lett.*, vol. 37, no. 20, pp. 4308–4310, Oct. 2012.

[19] H. Y. Choi, M. J. Kim, and B. H. Lee, "All-fiber Mach–Zehnder type interferometers formed in photonic crystal fiber," *Opt. Exp.*, vol. 15, no. 9, pp. 5711–5720, Apr. 2007.

[20] B. Dong, D. P. Zhou, and L. Wei, "Temperature insensitive all-fiber compact polarization-maintaining photonic crystal fiber based interferometer and its applications in fiber sensors," *J. Lightw. Technol.*, vol. 28, no. 7, pp. 1011–1015, Apr. 2010.
[21] K. K. Qureshi, Z. Y. Liu, H. Y. Tam, and M. F. Zia, "A strain sensor based on in-line fiber Mach–Zehnder interferometer in twin-core photonic crystal fiber," *Opt. Commun.*, vol. 309, no. 15, pp. 68–70, Nov. 2013.
[22] J. R. Zheng *et al.*, "Temperature and index insensitive strain sensor based on a photonic crystal fiber in line Mach–Zehnder interferometer," *Opt. Commun.*, vol. 297, no. 15, pp. 7–11, Jun. 2013.
[23] X. Xi, G. Wong, T. Weiss, and P. Russell, "Measuring mechanical strain and twist using helical photonic crystal fiber," *Opt. Lett.*, vol. 38, no. 24, pp. 5401–5404, Dec. 2013.
[24] S. Liu *et al.*, "Multilongitudinal mode fiber laser for strain measurement," *Opt. Lett.*, vol. 35, no. 6, pp. 835–837, Mar. 2010.
[25] L. Gao, L. Chen, L. Huang, and X. F. Chen, "Multimode fiber laser for simultaneous measurement of strain and temperature based on beat frequency demodulation," *Opt. Exp.*, vol. 20, no. 20, pp. 22 517–22 522, Sep. 2012.
[26] Z. B. Liu, Y. Li, Y. Liu, Z. W. Tan, and S. S. Jian, "A static axial strain fiber ring cavity laser sensor based on multimodal interference," *IEEE Photon. Technol. Lett.*, vol. 25, no. 21, pp. 2050–2053, Nov. 2013.
[27] J. Villatoro, V. Finazzi, V. P. Minkovich, V. Pruneri, and G. Badenes, "Temperature-insensitive photonic crystal fiber interferometer for absolute strain sensing," *Appl. Phys. Lett.*, vol. 91, no. 9, pp. 091109-1–091109-3, Sep. 2007.
[28] J. T. Zhou *et al.*, "Simultaneous measurement of strain and temperature by employing fiber Mach–Zehnder interferometer," *Opt. Exp.*, vol. 22, no. 2, pp. 1680–1686, Jan. 2014.